Available online at www.sciencedirect.com
ScienceDirect
Journal of Pharmaceutical and Biomedical Analysis 46 (2008) 274–281
JOURNAL OF PHARMACEUTICAL AND BIOMEDICAL ANALYSIS
www.elsevier.com/locate/jpba

Application of Raman microscopy and band-target entropy minimization to identify minor components in model pharmaceutical tablets

Effendi Widjaja *, Regina Kim Hong Seah

Process Science and Modeling, Institute of Chemical and Engineering Sciences, 1 Pesek Road, Jurong Island, Singapore 627833, Singapore

Received 31 May 2007; received in revised form 19 September 2007; accepted 21 September 2007
Available online 29 September 2007

Abstract

The aim of the current study is to establish a useful analytical technique to detect and identify minor components of pharmaceutical drug tablets using Raman microscopy and advanced multivariate data analysis method, namely band-target entropy minimization (BTEM). Model pharmaceutical tablets comprising four components with varying proportions were prepared with a custom press tooling after blending. One of the components, magnesium stearate, was made as a minor component, with weight percentages of 2%, 1%, 0.5%, and 0.2% in four model tablets. Raman point-by-point mapping was performed on an area of 200 μm × 200 μm using a near infrared laser source and a 50× objective lens with a step size of 5 μm in both the *x* and *y* directions. Advanced multivariate analysis, BTEM, was then performed on the Raman mapping data to recover all observable pure component spectra. BTEM was successfully applied to recover the pure component spectrum of magnesium stearate, which was present as a minor component (as low as 0.2 wt%) in the prepared tablet. The success of BTEM in identifying minor chemical species offers a new analytical technology for detecting impurities or any other minor components in pharmaceutical tablets.

Keywords: Minor components; Raman microscopy; Band-target entropy minimization (BTEM); Multivariate data analysis; Pharmaceutical tablet analysis

1. Introduction

In recent years, Raman microscopy has become one of the important analytical tools in the pharmaceutical industry due to its unique characteristics, such as non-invasive in nature, easy or no sample preparation, local investigation of solids, and simple instrument operation. Raman microscopy is built from the integration of spectroscopy and microscope. Coupled with a mapping technique via programmed movements of a microscope objective, it is able to simultaneously provide both spectral and spatial information of the sample under investigation. Therefore, this technique enables user to obtain the Raman band structures, which relate to chemical and morphological characters of the investigated materials as well as the chemical distribution of materials in two or three spatial dimensions. It is hence very useful for identifying chemical identities of active pharmaceutical ingredients (APIs), excipients, impurities and their locations within the solid dosage formulated products [1–3].

The collected Raman map data require further data processing in order to extract useful and meaningful chemical information. When *a priori* knowledge of chemicals being observed and selective information from single spectral channels are available, a univariate data analysis approach can be sufficient to reveal the spatial distribution of components. However, when selective information is not available due to highly overlapping spectra, multivariate data analysis approaches [4–7] are more effective to produce better quality spatial distribution of the observed components. A comparison study between univariate and multivariate approaches to generate Raman chemical images has been performed by Sasic et al. and their results showed that multivariate approach indeed outperformed univariate approach [8].

A more complicated case is encountered when *a priori* knowledge of one or a few or even all chemicals in a system is totally unavailable. The corresponding analysis becomes more complex and certainly requires more sophisticated data analysis

* Corresponding author. Tel.: +65 6796 3943; fax: +65 6316 6185.
E-mail address: effendi_widjaja@ices.a-star.edu.sg (E. Widjaja).

0731-7085/$ – see front matter © 2007 Elsevier B.V. All rights reserved.
doi:10.1016/j.jpba.2007.09.023

tool. Recently, various self-modeling curve resolution (SMCR) methods, which are multivariate data analysis techniques, are gaining more widespread application in analyzing spectroscopic imaging data [6,9–14]. Using SMCR techniques, it is possible to extract pure component spectra information and component spatial distribution without any *a priori* information about the composition of the object being mapped. For analyzing pharmaceutical tablet, Zhang et al. [6] used a multivariate curve resolution approach (Simplisma and alternating least squares) to recover pure component Raman spectra from a model tablet made from avicel, lactose, sodium benzoate, and magnesium stearate. Their results showed that three pure component Raman spectra of avicel, lactose, and sodium benzoate were well recovered; however, pure spectrum of magnesium stearate could not be successfully resolved due to its low quantity in the model tablet.

Unlike other SMCR techniques, band-target entropy minimization (BTEM) was developed especially to recover pure component spectra of species present at sub-ppm levels in a liquid system [15]. Initially, BTEM was applied to resolve pure component spectra from both non-reactive and reactive multicomponent liquid systems measured by FT-IR [15–19]. However, recently it has also been successfully applied to resolve pure component spectra of Raman data measured from solid-state chemical problems [20,21] and biological material [13,22].

Since BTEM utility is general, in the current contribution we aim to develop BTEM to be an effective analytical method to recover pure component spectra of minor components present in pharmaceutical solid tablets.

2. Experimental

2.1. Model pharmaceutical tablet

Four model pharmaceutical tablets comprising four components, i.e. acetaminophen (10–11.8 wt%), lactose (68 wt%), avicel (20 wt%), and magnesium stearate with varying proportions, were prepared with custom press tooling after blending. Magnesium stearate was assigned as a minor component, with weight percentages of 2%, 1%, 0.5%, and 0.2%, respectively. All chemicals were purchased from Sigma–Aldrich and were used without further purifications.

2.2. Raman microscopy

Raman mixture spectra were measured using a Raman microscope (InVia Reflex, Renishaw) equipped with near infrared enhanced deep-depleted thermoelectrically Peltier cooled CCD array detector (576 × 384 pixels) and a high grade Leica microscope. The Raman scattering was excited with a 785 nm near infrared diode laser and a 50× objective lens was used to collect the backscattered light. Raman point-by-point mapping with a step size of 5 μm in both the x and y directions was performed in an area of 200 μm × 200 μm. Scans were performed in an extended spectral window from 300 to 1800 cm^{-1} and acquisition time for each spectrum was around 30 s. The final

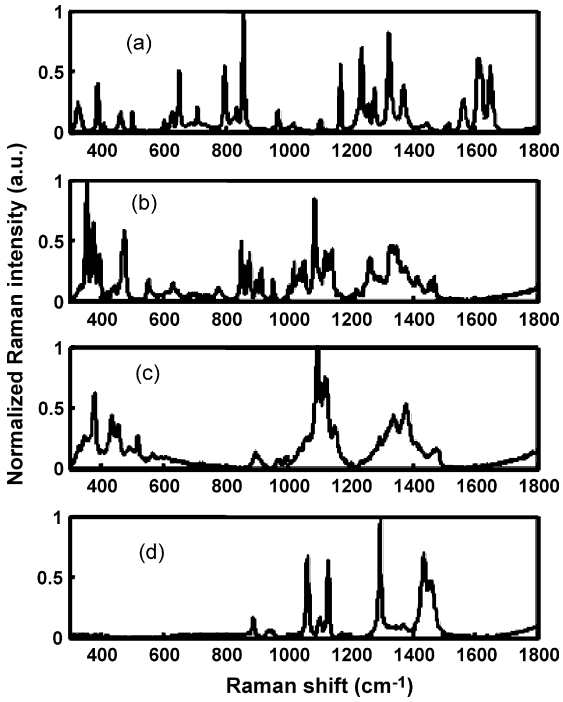

Fig. 1. Experimental pure reference Raman spectra: (a) acetaminophen, (b) lactose, (c) avicel and (d) magnesium stearate.

three-dimensional Raman imaging data cube collected from one experiment is of the format of 41 × 41 × 1588. The time required for one experiment is circa 800 min. Such huge time requirement is certainly one of the drawbacks of Raman point-mapping measurements. However, in future investigations, such time requirement can be much reduced by using Raman line-mapping measurement, in which one line consists of 20 spectra. As such, time requirement for one similar experiment can be reduced to only circa 40 min. Pure reference Raman spectra of acetaminophen, lactose, avicel, and magnesium stearate were obtained by measuring each pure sample using similar measurement conditions and are shown in Fig. 1.

2.3. Spectral preprocessing

The Raman image data were first reorganized from a three-way array to a conventional two-way array (pixel × channel) for processing. Since the raw Raman spectra acquired from these model tablets were a combination of Raman scattering signals, spikes due to cosmic rays, and some autofluorescence background, some spectral preprocessing was needed to generate Raman spectral alone. Spikes were removed in the first step followed by baseline correction using third order modified polynomial fitting [23].

2.4. Band-target entropy minimization (BTEM)

One powerful and recently developed SMCR method is band-target entropy minimization (BTEM) [19], which primary utility is to reconstruct pure component spectra from a set of multicomponent mixture spectra without using any spectral library or any

a priori knowledge. This relatively new SMCR technique finds its origin in Shannon's information entropy concept [24], which can be defined as a measure of choice and uncertainty [25], where uncertainty means random and disordered information. By this definition, lowering information entropy will result in a more organized and simpler system. In curve resolution, it is assumed that the recovered pure component spectra will have simpler and less line shape, and thus less entropy than the experimental mixture spectra. Minimizing entropy will also localize the spectral information around the major bands and maximize the number of zero elements in the recovered spectrum. In summary, entropy minimization techniques in general and BTEM in particular, aim to search for the simplest (irreducible) underlying patterns in the spectroscopic observations. The potential usefulness of entropy minimization for more general pattern recognition has been noted elsewhere by Watanabe [26].

Let $\mathbf{I}_{k\times\nu}$ represent the Raman intensity in the consolidated spectroscopic data matrix where k denotes the number of spectra taken, and ν denotes the number of data channels associated with the spectroscopic range. The experimental intensities $\mathbf{I}_{k\times\nu}$ have a bilinear data structure and can be described as a product of two sub-matrices, namely, the concentration matrix $\mathbf{C}_{k\times s}$ and the Raman pure component scattering coefficient matrix $\mathbf{J}_{s\times\nu}$ (where s denotes number of observable species in the chemical mixture). Accordingly, the associated error matrix $\boldsymbol{\varepsilon}_{k\times\nu}$ contains both experimental error and model error (non-linearities) [27]:

$$\mathbf{I}_{k\times\nu} = \mathbf{C}_{k\times s}\mathbf{J}_{s\times\nu} + \boldsymbol{\varepsilon}_{k\times\nu} \tag{1}$$

The BTEM algorithm proceeds by first decomposing $\mathbf{I}_{k\times\nu}$ into its singular vectors using singular value decomposition (SVD). This is then followed by the appropriate transformation of right singular vectors, $\mathbf{V}^{\mathrm{T}}$, into physically meaningful pure component spectra.

$$\mathbf{I}_{k\times\nu} = \mathbf{U}_{k\times k}\Sigma_{k\times\nu}\mathbf{V}^{\mathrm{T}}_{\nu\times\nu} \tag{2}$$

Unlike other SMCR methods, BTEM is uniquely developed to resolve one pure spectrum at a time. The number of right singular vectors, z, taken for inclusion in the transformation is usually much larger than s due to the non-linearities present (non-stationary spectral characteristics). The number z is usually determined by identifying the vectors which possess localized signals of clear physical significance and retaining these, while discarding the vectors that are more-or-less randomly distributed noise.

$$\widehat{\mathbf{J}}_{1\times\nu} = \mathbf{T}_{1\times z}\mathbf{V}^{\mathrm{T}}_{z\times\nu} \tag{3}$$

To extract a pure spectrum $\widehat{\mathbf{J}}_{1\times\nu}$, a selected band present and visibly observed in the first few $\mathbf{V}^{\mathrm{T}}$ vectors that are plausibly associated with pure component spectral bands is targeted. The BTEM algorithm then retains this feature, and at the same time, returns an entire spectrum, which has the minimum entropy. This routine is repeated for all important observable physical features in the selected $\mathbf{V}^{\mathrm{T}}$ vectors. Criterion for selecting the band targets is simple. A user of this algorithm may first interactively set the base point of noise level observed in the first few $\mathbf{V}^{\mathrm{T}}$ vectors. Then, the observed spectral features in the first few $\mathbf{V}^{\mathrm{T}}$ vectors with the absolute intensity above this base point are selected as band-targets for BTEM. Since there are many repetitive spectral features selected as band targets, the number of band-targets for BTEM analysis can be further reduced. A superset of reconstructed spectra is then obtained and this set is again further reduced by the user to eliminate redundancies due to noise reconstruction and repetitive reconstructed pure component spectra. Finally, this analysis results in an enumeration of all observable pure component spectra.

As part of the process, the resulting pure spectral patterns are returned in a normalized form. When all normalized observable pure component spectra have been reconstructed, the relative concentration values are recovered by projection onto the original data set. The score images for each pure component that represent its spatial distribution can be obtained by folding back the two-way array data into three-way array data. For detailed descriptions of the BTEM algorithm, the readers are referred to Refs. [16–19].

3. Results and discussion

The four collected Raman image data with different proportions of magnesium stearate in the model tablets (0.2–2 wt%) were preprocessed and analyzed using BTEM.

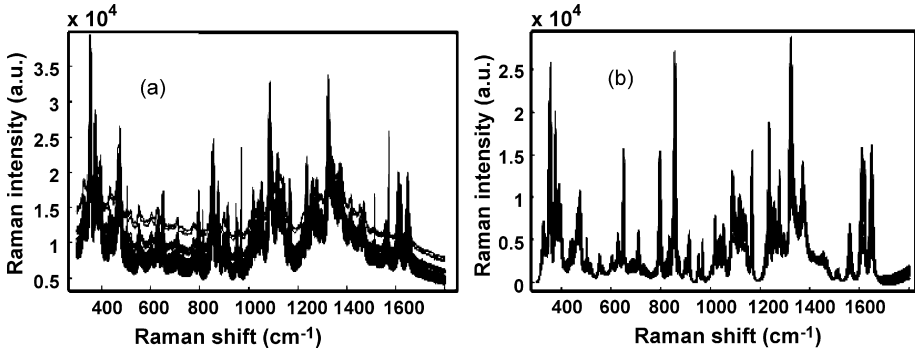

Fig. 2. (a) Raw Raman spectra taken from a model tablet having 2 wt% magnesium stearate before any spectral preprocessing. (b) Raman spectra after spectral preprocessing.

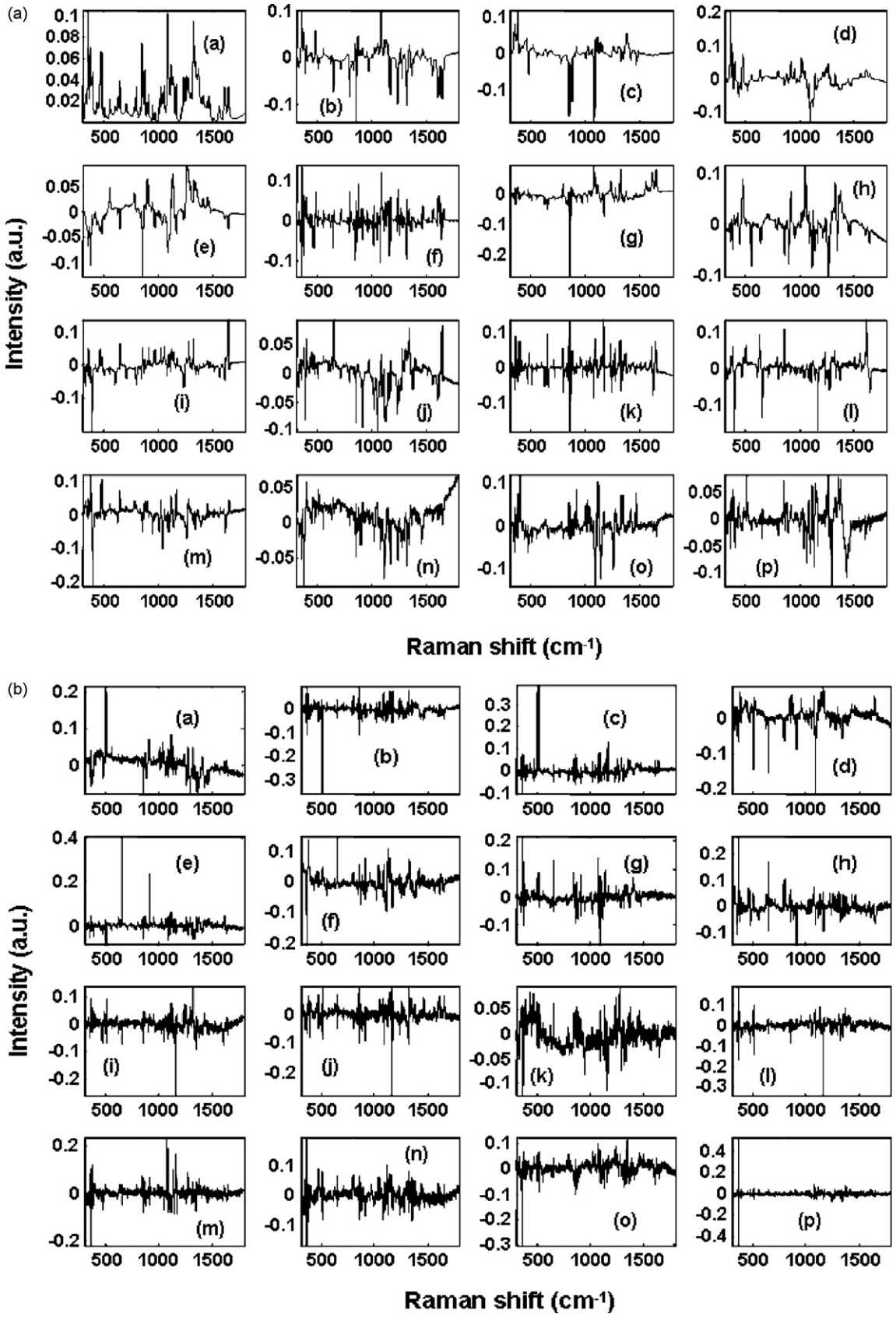

Fig. 3. (a) The first 16 right singular vectors of the $\mathbf{V}^{T}$ matrix: (a) 1st vector, (b) 2nd vector, (c) 3rd vector, . . ., (p) 16th vector; (b) The second 16 right singular vectors of the $\mathbf{V}^{T}$ matrix: (a) 17th vector, (b) 18th vector, (c) 19th vector, . . ., (p) 32nd vector.

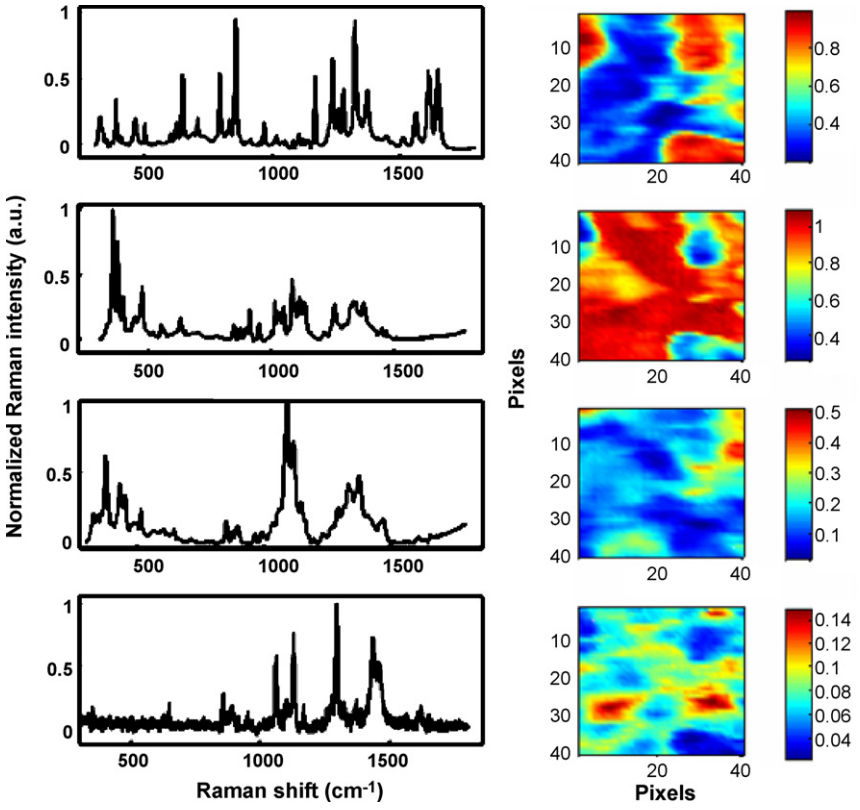

Fig. 4. Pure component Raman spectra estimates and their associated score images obtained via BTEM from a model tablet having 2 wt% magnesium stearate. The axes of score images are in pixels and can be directly correlated to distance by multiplying each pixel with 5 μm: (a) acetaminophen, (b) lactose, (c) avicel and (d) magnesium stearate.

3.1. Pure component spectral reconstruction of Raman data taken from a model tablet having 2 wt% magnesium stearate

Fig. 2a presents one of the raw Raman data taken from a model tablet having 2 wt% magnesium stearate after unfolding the Raman image data into two-way array data (only the first 121 Raman spectra are shown). As can be seen, typical spikes due to cosmic rays and background due to fluorescence are present. After removing spikes and performing baseline correction, clear Raman spectra are shown in Fig. 2b.

Singular value decomposition was performed on the 1681 Raman spectra (41 × 41 pixels) and the resulting first 32 right singular vectors of this data matrix were shown in Fig. 3a and b. These figures clearly show that although there are only four components in this model tablet, there are still many significant spectral features related to these four components visible in the first 16 right singular vectors. More noise contributions are noticed in the next four vectors although they still possess some localized signals. Vectors 21–31 are primarily noise but the noise is structured and heteroscedasticly distributed. The remaining vectors are essentially only white noise. A closer examination was performed on the right singular vectors. In the first 10 vectors, most spectral features are associated with major components, i.e. acetaminophen, lactose, and avicel, and it is difficult to observe any magnesium stearate spectral features. A significant spectral feature of magnesium stearate at 1296 cm^{-1}, however, can be found in the 16th right singular vector. This observation shows that singular value decomposition is able to resolve some chemical signals of minor components provided that sufficient variation is present. In addition, this observation is also in agreement with a previous study performed by Hasegawa [28]. Hasegawa suggested that principal component analysis has a great potential for resolving the spectrum of a minor chemical species even if it is present within a large quantity of other species. The spectral feature at 1296 cm^{-1} found in the 16th right singular vector is thus used as one of the band-targets for the BTEM analysis.

Exhaustive band targeting for all important observable physical features in the selected $\mathbf{V}^T$ vectors as mentioned in the BTEM procedure was performed. A superset of reconstructed pure component spectra was obtained and this set was further reduced to eliminate the redundancies. Finally, after reduction we reconstructed four pure component spectra, which were resulted from four band-targeted features at 1323–1326, 354–358, 1092–1098, 1294–1300 cm^{-1}.

Since the Raman component spectra generally have many narrow features, the objective function used in this BTEM analysis is the summation of the spectral second derivatives plus the summation of band areas. The numbers of right singular vectors taken for these spectral reconstructions were 15, 15, 15, and 50 for the corresponding resolved pure component spectral estimates of acetaminophen, lactose, avicel, and magnesium stearate, respectively. The need for more numbers of right singular vectors to reconstruct a pure component spectrum of a

minor component is because its spectroscopic signal is found mostly at higher right singular vectors. The relative contribution of each component in each pixel of the area being imaged was then deduced by projecting back the pure component spectral estimates to the original mixture spectra. These pure component spectral estimates and their score images are presented in Fig. 4.

By visual inspection, it can be observed that there is a considerable correspondence between the BTEM reconstructed spectra and the measured pure reference spectra. The relative intensities of the Raman bands and their positions are quite similar in most cases. The only minor discrepancies that can be observed are the decrease of relative intensities of lactose especially in the region of 800–1200 cm^{-1} and the lower signal-to-noise ratio of the BTEM reconstructed magnesium stearate. The discrepancy of lactose might be due to some crystallinity changes [29] caused by grinding and direct compression when the model tablets were prepared and these changes were detectable by Raman spectroscopy. The lower signal-to-noise ratio of magnesium stearate (only 2 wt%) compared to major components, however, was expected. Since there was only 2% weight of magnesium stearate in this model tablet, Raman signals of magnesium stearate were much lower compared to Raman signals from major components and the signals were just above noise signals.

3.2. Pure component spectral reconstruction of Raman data taken from model tablets having less than 2 wt% magnesium stearate

The selection of the number of right singular vectors used for BTEM analysis is quite critical, particularly when BTEM is used to reconstruct the pure spectra of minor components. In general, BTEM only requires 12–30 right singular vectors for spectral reconstruction of major components in a system having 4–10 species [13,18]. However, when BTEM is used to deal with minor component spectral reconstruction, the number of right singular vectors, z, to be included in the rotation will determine the quality of the reconstructed pure spectrum. If the number of z vectors used for reconstruction is too low, spectral information on the component corresponding to the targeted band in the later vectors is not included. This will result in the reconstructed pure spectrum containing some spectral peaks or bands associated with other components. On the other hand, if too many right singular vectors are taken, the optimization burden during spectral reconstruction will increase, and hence there is a danger of over-fitting.

In a previous study, we have shown that a small test could be developed to determine the number of right singular vectors to include in the spectral reconstruction [13]. This test is performed by examining the weight distribution of $\mathbf{T}_{1\times z}$ elements versus the number of right singular vectors. Again, in this current study, we used various numbers of right singular vectors ranging from 30 to 120 vectors to reconstruct the pure component spectrum estimate of magnesium stearate from a model tablet having 1% weight magnesium stearate. Similar band-target at 1294–1300 cm^{-1} associated with magnesium stearate spectral feature was again used in these reconstructions. The resulting

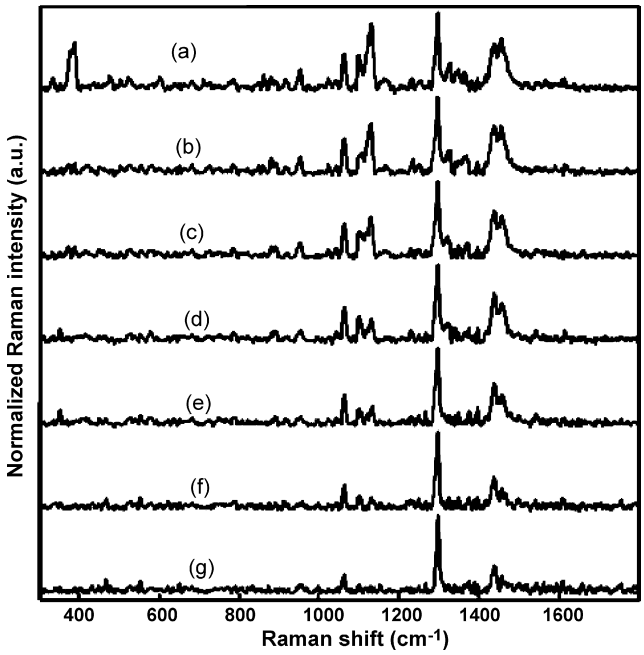

Fig. 5. Pure component Raman spectra estimate of magnesium stearate recovered via BTEM using: (a) 30 $\mathbf{V}^T$ vectors, (b) 40 $\mathbf{V}^T$ vectors, (c) 50 $\mathbf{V}^T$ vectors, (d) 60 $\mathbf{V}^T$ vectors, (e) 75 $\mathbf{V}^T$ vectors, (f) 100 $\mathbf{V}^T$ vectors and (g) 120 $\mathbf{V}^T$ vectors.

BTEM estimates and the plot of the optimum elements of the $\mathbf{T}_{1\times z}$ vector versus number of right singular vectors that determines the weight distribution for the linear combination of the z vectors are shown in Figs. 5 and 6, respectively. In addition, Fig. 7 shows the experimental pure component Raman spectrum of magnesium stearate for comparison.

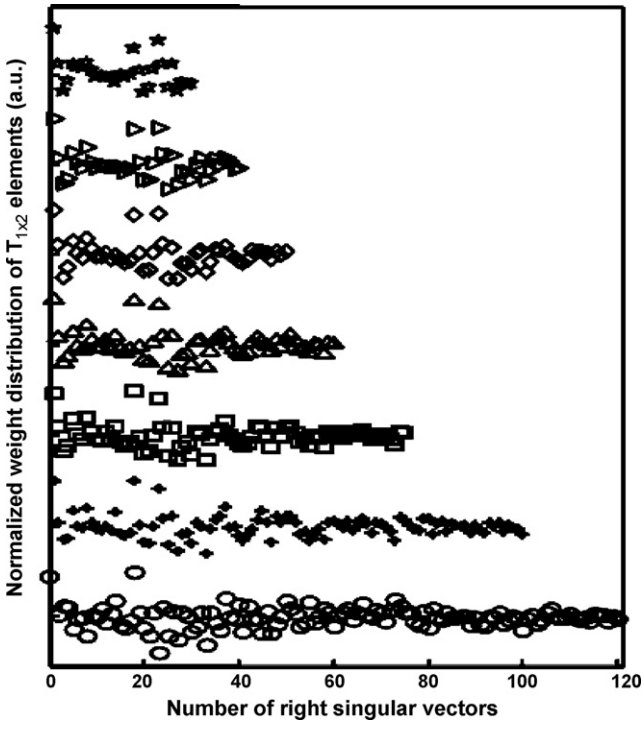

Fig. 6. Weight distribution of normalized optimum $\mathbf{T}_{1\times z}$ vs. number of right singular vectors, z.

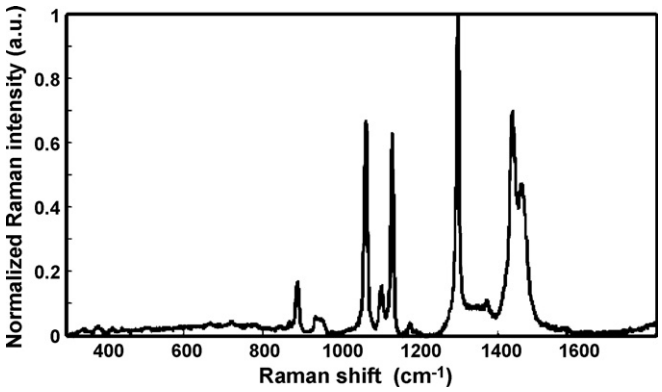

Fig. 7. The experimental pure component Raman spectrum of magnesium stearate.

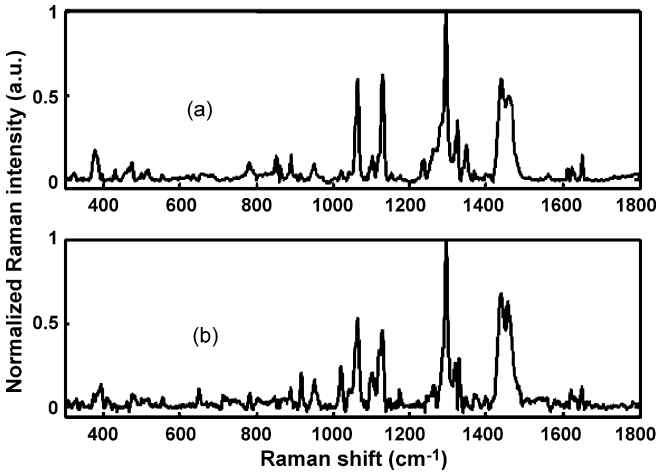

Fig. 8. Pure component Raman spectra estimate of magnesium stearate recovered via BTEM using 60 $\mathbf{V}^{\mathrm{T}}$ vectors from model tablet having. (a) 0.5 wt% magnesium stearate and (b) 0.2 wt% magnesium stearate.

Comparing Figs. 5 and 7, BTEM estimates of magnesium stearate reconstructed from 30 to 40 right singular vectors still contain some spectral features, which are not associated with magnesium stearate. For 30 and 40 vectors rotation, it can also be seen (Fig. 6) that $\mathbf{T}_{1\times z}$ elements are scattered and do not converge to zero. This result shows that more z vectors are needed in the rotation because some spectral information corresponding to the targeted band is still present in the higher number of right singular vectors. When 50 vectors were included in the rotation, the weight distribution of $\mathbf{T}_{1\times z}$ elements seems to start converging towards zero and the reconstructed BTEM estimate is now almost similar to experimental features of magnesium stearate, although some spectral noises and small discrepancies can still be found. For the higher number of z vectors (60, 75, 100 and 120) rotation, the weight distribution of $\mathbf{T}_{1\times z}$ elements is also shown to be converging towards zero. Although the most significant peak of magnesium stearate at 1296 cm^{-1} was still reconstructed in all BTEM estimates using 60–120 vectors rotation, some associated peaks belonging to magnesium stearate began to disappear, particularly when more than 60 vectors were used (Fig. 5). Although the inclusion of right singular vectors containing distributed random noise in the rotation improves the signal-to-noise ratio of the recovered spectra, at the same time, when too many vectors are taken, over-fitting may occur. The best BTEM estimate of magnesium stearate that most resembles the pure reference (Fig. 7) was from 50 to 60 vectors rotation. Hence, if a truly unknown minor component is encountered, spectral reconstruction based on progressive number of $\mathbf{V}^{\mathrm{T}}$ vectors can be carried out. The smallest number of $\mathbf{V}^{\mathrm{T}}$ vectors required to achieve the convergence of the elements of the rotation matrix can be a good indicator of the number of vectors to use in resolving the pure spectrum of the minor component.

In order to further evaluate the capability of BTEM to identify and recover the pure spectrum of a minor component, BTEM was used to analyze two other model tablets, which contained 0.5 wt% and 0.2 wt% magnesium stearate, respectively. Similar band target at 1294–1300 cm^{-1} was used and 60 right singular

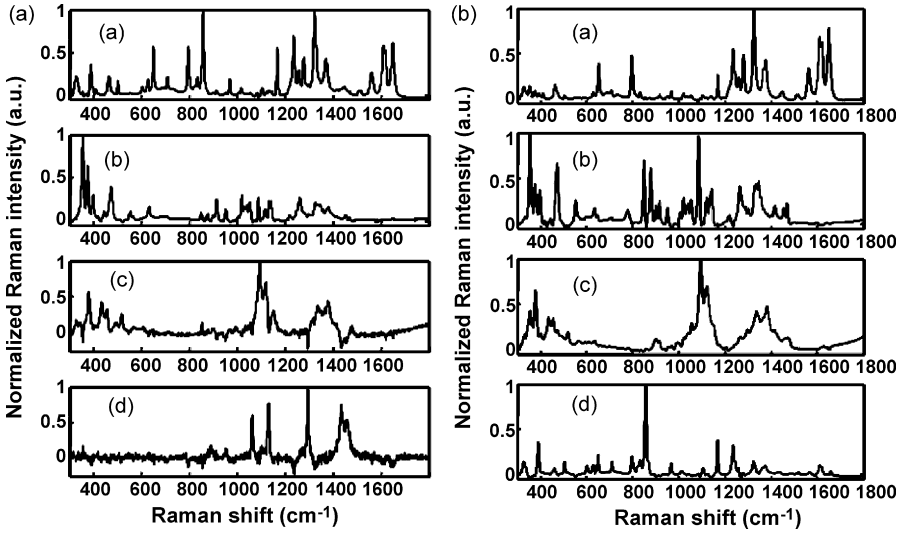

Fig. 9. (a) Pure component Raman spectra estimates recovered via Simplisma from a model tablet having 2 wt% magnesium stearate: (a) acetaminophen, (b) lactose, (c) avicel and (d) magnesium stearate. (b) Pure component Raman spectra estimates recovered via Simplisma from a model tablet having 1 wt% magnesium stearate: (a) partial features of acetaminophen, (b) lactose, (c) avicel and (d) another partial features of acetaminophen.

vectors were rotated. The reconstructed pure spectra of magnesium stearate are shown in Fig. 8. Although some uncorrelated bands, which belong to other components were also simultaneously reconstructed in these estimates, these bands were not significant and their intensities were quite low compared to the bands associated to magnesium stearate. All significant bands of magnesium stearate were recovered and the signal-to-noise ratio of BTEM estimates was about 20. These results show that the BTEM algorithm is effective for detecting such minor components in pharmaceutical tablets with concentration level as low as 0.2 wt%.

3.3. Comparison with Simplisma technique

Simplisma technique was also employed to extract the pure component spectra of the model tablets having 2 wt% and 1 wt% magnesium stearate. Simplisma was first proposed by Windig and Guilment [30]. It is performed by searching the potentially pure variables in the mixture spectral data matrix. Pure variable is defined as variable which spectral intensity contribution is assumed from only one or almost one component in a mixture. Therefore, if pure variables of all components in the mixture are known, the concentration profiles of all observable components can be estimated. These estimates will then be used to resolve the pure component spectra of the mixture spectra based on the linear relationship of spectral data via multiple linear regressions. The offset value, which is required in Simplisma technique, was obtained through trial and error.

In the current studies, we used the offset value of 10% of the maximum value in the mean spectrum, which is similar to the value suggested in literature [31]. The resulting pure component spectra estimates are shown in Fig. 9a and b. For the model tablet with 2 wt% magnesium stearate, all pure component spectra could be reconstructed. However, as can be seen in Fig. 9a, there are some spectral distortions, particularly for pure component spectral estimates of lactose, avicel, and magnesium stearate. In addition, some negative spectral interference from other components could also be seen for avicel and magnesium stearate estimates. For model tablet having 1 wt% magnesium stearate, as can be seen in Fig. 9b, only pure component spectra of lactose and avicel were well reconstructed. Pure component spectrum estimate of acetaminophen was separated into two individual spectra and pure component spectrum of magnesium stearate was totally unrecovered. The poor recovery result of minor component using Simplisma was expected, since the signal intensities of magnesium stearate were just above the noise level. Simplisma technique was also used to recover the pure component spectra of the model tablets having 0.5 wt% and 0.2 wt% magnesium stearate. Since similar results were obtained, in which only pure component spectra of major components were recovered, the resulting estimates via Simplisma for these two model tablets are not shown.

4. Conclusions

The results from this study demonstrate that the combination of Raman microscope and BTEM algorithm is a powerful technique to recover pure component spectrum of minor components in pharmaceutical tablets, even at a concentration as low as 0.2 wt%. This novel analytical technique opens new possibilities to detect and identify impurities and counterfeits, which are often present in minor amounts.

References

[1] S. Wartewig, R.H.H. Neubert, Adv. Drug Del. Rev. 57 (2005) 1144–1170.
[2] T. Kojima, S. Onoue, N. Murase, F. Katoh, T. Mano, Y. Matsuda, Pharm. Res. 23 (2006) 806–812.
[3] J. Breitenbach, W. Schrof, J. Neumann, Pharm. Res. 16 (1999) 1109–1113.
[4] A.C. Jorgensen, I. Miroshnyk, M. Karjalainen, K. Jouppila, S. Siiria, O. Antikainen, J. Rantanen, J. Pharm. Sci. 95 (2006) 906–916.
[5] A. Jorgensen, J. Rantanen, M. Karjalainen, L. Khriachtchev, E. Rasanen, J. Yliruusi, Pharm. Res. 19 (2002) 1285–1291.
[6] L. Zhang, M.J. Henson, S.S. Sekulic, Anal. Chim. Acta 545 (2005) 262–278.
[7] S. Sasic, D.A. Clark, Appl. Spectrosc. 60 (2006) 494–502.
[8] S. Sasic, D.A. Clark, J.C. Mitchell, M.J. Snowden, Analyst 129 (2004) 1001–1007.
[9] S. Sobanska, G. Falgayrac, J. Laureyns, C. Bremard, Spectrochim. Acta 64 (2006) 1102–1109.
[10] B.K. Lavine, C.E. Davidson, J. Ritter, D.J. Westover, T. Hancewicz, Microchem. J. 76 (2004) 173–180.
[11] Y. Batonneau, S. Sobanska, J. Laureyns, C. Bremard, Environ. Sci. Technol. 40 (2006) 1300–1306.
[12] K. Artyushkova, J.E. Fulghum, J. Electron Spectrosc. Relat. Phenom. 121 (2001) 33–55.
[13] E. Widjaja, N. Crane, T.-S. Chen, M.D. Morris, M.A. Ignelzi Jr., B.R. McCreadie, Appl. Spectrosc. 57 (2003) 1353–1362.
[14] H. Fenniri, O. Terreau, S. Chun, S.J. Oh, W.F. Finney, M.D. Morris, J. Comb. Chem. 8 (2006) 192–198.
[15] C.Z. Li, E. Widjaja, W. Chew, M. Garland, Angew. Chem. 41 (2002) 3784–3789.
[16] W. Chew, E. Widjaja, M. Garland, Organometallics 21 (2002) 1982–1990.
[17] E. Widjaja, C.Z. Li, M. Garland, Organometallics 21 (2002) 1991–1997.
[18] E. Widjaja, C.Z. Li, W. Chew, M. Garland, Anal. Chem. 75 (2003) 4499–4507.
[19] E. Widjaja, PhD Thesis, National University of Singapore, Singapore, 2002.
[20] L.R. Ong, E. Widjaja, R. Stanforth, M. Garland, J. Raman Spectrosc. 34 (2003) 282–289.
[21] S.Y. Sin, E. Widjaja, L.E. Yu, M. Garland, J. Raman Spectrosc. 34 (2003) 795–805.
[22] N.J. Crane, V. Popescu, M.D. Morris, P. Steenhuis, M.A. Ignelzi, Bone 39 (2006) 434–442.
[23] C.A. Lieber, A. Mahadevan-Jansen, Appl. Spectrosc. 57 (2003) 1363–1367.
[24] C.E. Shannon, Bell Sys. Tech. J. 3 (1948) 379–423.
[25] C.E. Shannon, W. Weaver, The Mathematical Theory of Communication, The University of Illinois Press, Urbana, IL, 1949.
[26] S. Watanabe, Pattern Recogn. 13 (1981) 381–387.
[27] M. Garland, E. Visser, P. Terwiesch, D.W.T. Rippin, Anal. Chim. Acta 351 (1997) 337–358.
[28] T. Hasegawa, Trends Anal. Chem. 20 (2001) 53–64.
[29] F.P.A. Fabbiani, C.R. Pulham, Chem. Soc. Rev. 35 (2006) 932–942.
[30] W. Windig, J. Guilment, Anal. Chem. 63 (1991) 1425–1432.
[31] W. Windig, B. Antalek, J.L. Lippert, Y. Batonneau, C. Bremard, Anal. Chem. 74 (2002) 1371–1379.